Ultra-compact micro-electro-mechanical laser beam scanner for augmented reality applications

Reitterer, Jörg, Chen, Zhe, Balbekova, Anna, Schmid, Gerhard, Schestak, Gregor, et al.

Jörg Reitterer, Zhe Chen, Anna Balbekova, Gerhard Schmid, Gregor Schestak, Faraj Nassar, Manuel Dorfmeister, Matthias Ley, "Ultra-compact micro-electro-mechanical laser beam scanner for augmented reality applications," Proc. SPIE 11765, Optical Architectures for Displays and Sensing in Augmented, Virtual, and Mixed Reality (AR, VR, MR) II, 1176504 (27 March 2021); doi: 10.1117/12.2576704

SPIE.

Event: SPIE AR VR MR, 2021, Online Only

Ultra-compact micro-electro-mechanical laser beam scanner for augmented reality applications

Jörg Reitterer*[a], Zhe Chen[a], Anna Balbekova[a], Gerhard Schmid[a], Gregor Schestak[a], Faraj Nassar[a], Manuel Dorfmeister[a], Matthias Ley[a]
[a]TriLite Technologies GmbH, Frankenberggasse 13, 1040 Vienna, Austria, Europe

ABSTRACT

Laser beam scanners (LBS) are an emerging micro-display technology for augmented reality (AR) head-mounted displays (HMD), enabling small-form-factor and low-power display units with large field of view (FOV) and daylight-bright luminance, that are compatible with a large range of optical combiner technologies such as waveguide or holographic combiners. We have developed an ultra-compact and lightweight LBS comprising an integrated laser module, a single 2D micro-electro-mechanical systems (MEMS) mirror, and a molded interconnect device (MID). The compact integrated laser module contains red, green, and blue (RGB) semiconductor laser diodes (LDs) and a common system of microlenses for beam collimation, all enclosed in a single hermetically sealed package. The three LDs are mounted onto a single submount using a novel high-precision laser die bonding technique. This high-precision LD placement allows the use of collimation lenses that collimate all three laser beams simultaneously in contrast to separate lenses with additional active alignment steps for each color. No additional optical components such as mirrors and dichroic beam combiners are required—instead, the color channels are overlapped on a pixel-by-pixel basis by a "software beam combination" laser pulse timing algorithm. Both laser module and MEMS mirror are assembled on an MID with printed circuit board (PCB), which is connected to a driver board including video interface. We also give an outlook to future generations of fully mass manufacturable LBS systems with even smaller form factor.

Keywords: Laser beam scanners, LBS, MEMS, AR, MR, XR, HMD, micro-displays

1. INTRODUCTION

Optical architectures of see-through HMDs for AR applications consist of two main components: Micro-display engines for displaying the augmented image content and combiner optics for redirecting the image information and presenting it to a viewer's eye. Satisfying the requirements of all-day wearable and daylight-bright consumer AR devices in terms of size, weight[1], and image quality[2,3], imposes substantial challenges on both micro-display engines and combiner optics[4,5]. While for the latter component some thin and lightweight solutions have already been developed, such as free-space holographic element (HOE)[6,7,8] or waveguide optical combiners[9,10], the micro-display engines remain to be a major hurdle for realizing HMDs as lightweight as the eyewear of today[11].

There are two main categories of micro-display engines used in AR applications: panel-based and scanner-based optical engines[12]. Panel-based display engines consist of a two-dimensional (2D) array of pixels, which either requires external illumination, e.g., in the case of liquid-crystal on silicon (LCoS)[13] or digital light processing (DLP) displays[14], or is self-emissive, e.g., organic light-emitting diode (OLED)[15,16] or micro light emitting diode (mLED) displays[17,18]. One of the major downsides of any panel-based architecture is that the minimum pixel size is limited due to various manufacturing and efficiency constraints, also limiting the minimum panel size for a given image resolution. Since collimation optics are required to couple the light emitted by the display to the optical combiner, the minimum panel size also limits the compactness of collimation optics for a given target FOV and image resolution. These inherent pixel size limitations therefore result in a poor scaling of panel-based displays in terms of size and weight—especially for future wide FOV systems[19].

Scanner-based optical engines such as LBS systems deflect laser beams using moveable MEMS mirrors and display individual pixels of the image in a time-sequential manner. Since there is no object plane as in panel-based displays, the

*reitterer@trilite-tech.com; phone +43 1 947 5371; www.trilite-tech.com

Optical Architectures for Displays and Sensing in Augmented, Virtual, and Mixed Reality (AR, VR, MR) II,
edited by Bernard C. Kress, Christophe Peroz, Proc. of SPIE Vol. 11765, 1176504
 · doi: 10.1117/12.2576704

system is not limited explicitly by the law of etendue, resulting in substantial advantages in terms of display engine size and weight. Other advantages of LBS over panel-based displays include higher brightness, higher contrast, lower power consumption, larger FOV, lower optical distortions, and lower video-in to retina latency[19,20,21,22].

Due to the scanning nature of LBS, individual pixels are also not confined to a pre-defined grid but can be precisely redistributed across the FOV by timing the corresponding laser pulses[23], allowing for perfectly calibrated images presented to the viewer's eye even when elements in the optical path, e.g., optical combiners, introduce distortions to the image. Another unique property of LBS is that the display engine is focus-free since the laser beams are typically collimated before they are delivered to the scanning MEMS mirror. Depending on the optical combiner used in the HMD system, this can enhance the viewer's visual comfort[24].

In this paper, we present an ultra-compact LBS for AR applications. The LBS consists of three main components: an integrated laser module, a MEMS mirror, and a hybrid MID/PCB mounting platform. The laser module contains three different laser diode chips—one each for red, green, and blue—and beam collimation optics, all enclosed in a single hermetically sealed package. In our LBS system, no RGB beam combiner is required since the inherent angular offset of the three laser beams is eliminated by proprietary multi-parameter laser timing algorithms, which substantially reduces size and weight of the laser module. The MEMS mirror incorporated into the system is a single gimballed mirror that can deflect the laser beams in two orthogonal directions. Both laser module and MEMS mirror are mounted onto a hybrid MID-PCB platform.

This article is organized as follows: The ultra-compact RGB laser module with integrated collimation optics is introduced in Section 2. Section 3 describes the architecture of the complete LBS including laser module, MEMS mirror, and MID. In Section 4 the driving electronics architecture is discussed. Section 5 describes the design and evaluation of a demonstrator including key specifications.

2. INTEGRATED RGB LASER LIGHT MODULE

Size and weight of the complete HMD system and its individual components such as the display engines play pivotal roles in a user's AR experience[12]. For LBS micro-displays, this means that the laser module containing red, green, and blue laser diodes (LD) is required to be as compact and lightweight as possible. In state-of-the-art LBS systems, transistor outline (TO) packaged RGB LDs are used for illumination. However, the size of TO packaged LDs (smallest diameter of commercialized available TO LD package is 3.8 mm) limits the further miniaturization of the light module.

State-of-the-art LBS systems contain a light module where spatially separated RGB laser beams are combined before being delivered to a scanning mirror[25,26]. Thus, all RGB beams can be subsequently redirected from the mirror and directed to a screen, an observer, or an optical combiner (e.g., waveguide or holographic combiner). There are two main light module architecture approaches. The first one is the most common and it uses a system of mirrors or prisms with dichroic coatings allowing selective reflection and transmission of collimated RGB laser beams depending on a wavelength (Figure 1(a)). Those systems demand additional space in the light module and require precise assembly and alignment processes. The second approach allows for more compact laser modules, as it does not require any additional optical elements to combine RGB beams (Figure 1(b)). In such a system, non-coaxial beams are delivered to the mirror and a so-called "software beam combination" is applied. Here, the collimation optics are designed to achieve a desired beam tilting angle α so that the laser beams intersect at the MEMS mirror plane. We have developed the so-called TriLite Calibration Module to compensate the beam pointing angles of red, green, and blue laser beams and these three colors can be co-registered by software, without any hardware beam combiners and complex alignment processes (cf. Section 4).

In this research, an integrated RGB light module, containing red, green, and blue LDs, a fast axis collimator (FAC), a slow axis collimator (SAC), a common aluminum nitride (AlN) submount and base plate and a Kovar package are developed[24,27]. The schematic of the system can be seen in Figure 2(a). The three LDs are mounted onto a common submount together with FAC and SAC, which are two orthogonal plano-convex acylinder and cylinder micro-lenses for separate collimation of divergent laser diode beams in fast and slow axis, respectively. Only one common FAC lens and one common SAC lens are used for collimation of three laser beams. In order to compensate wavelength-dependent lens back focal length, the LD dies were shifted accordingly with respect to the light propagation direction (z-direction). The SAC lens consists of three segments which form a monolithic array of cylindrical lenses.

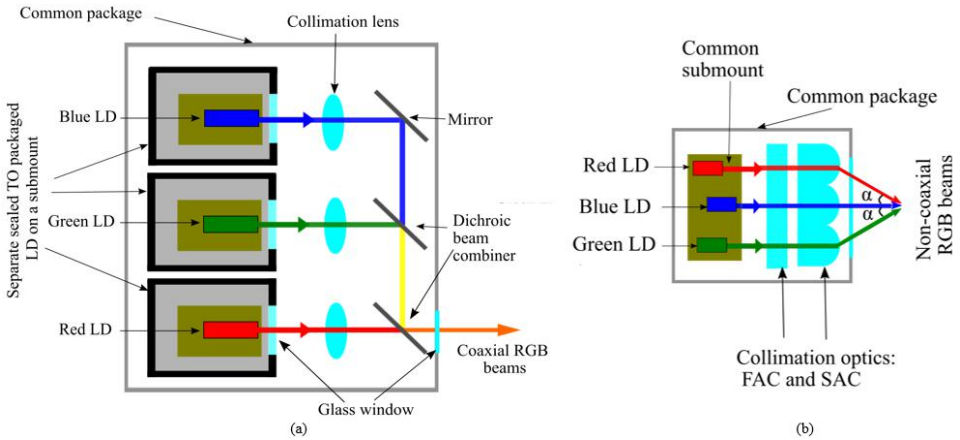

Figure 1. (a) State-of-the-art laser module with separate hermetically sealed RGB LDs, collimation optics, and dichroic beam combiner system and (b) integrated RGB laser module a with a common hermetically sealed package containing RGB LDs on a single submount and common collimation optics.

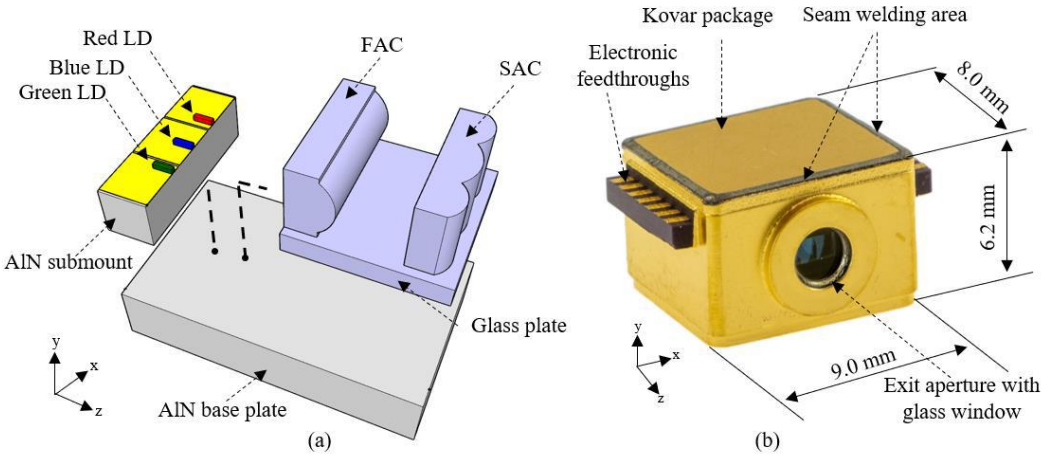

Figure 2. (a) Basic schematic and (b) package of the integrated RGB laser light module.

All components are enclosed in the single hermetically sealed Kovar package applying a seam welding process (cf. Figure 2(b)). The outer package dimensions are 9.0 mm x 8.0 mm x 6.2 mm. The collimated RGB beams exit the light package through the anti-reflection-coated glass window on the side of the Kovar package. The total volume of the light module is 0.45 cm^3 and the weight is 1.83 g. The module is electrically connected to the driving electronics via two feedthroughs on either side of the package. Inside the light module, the red, green, and blue LDs are electrically connected to the inner part of the feedthroughs via a wire bonding technique. The outer dimensions of future versions of the light module can be reduced even further based on specific requirements. Furthermore, additional components such as photodiodes, thermistors, RGB beam combiners, or optical attenuators can be integrated into the light module package as well.

In the assembly procedure, the LD dies are bonded to the submount using a passive alignment process with sub-µm accuracy of the three emission points of the red, green, and blue LDs in *x*-, *y*-, and *z*-directions. This high accuracy enables the possibility of collimating all three colors using common collimators (one common FAC collimator and one common SAC collimator). After mounting a supporting glass plate onto the base plate, the FAC is actively aligned while measuring the optical performance of the collimated laser beams. An ultra-low-shrinkage UV-curable adhesive is applied in the alignment procedure, followed by the UV-curing process. Finally, the SAC is actively aligned and UV-curing of the SAC is implemented. Alternatively, FAC and SAC can be combined into one monolithic lens. Comparing with the conventional approach of collimation (shown in Figure 1(a)), which typically requires three to six individual lenses for beam collimation, our approach requires less lens components and less active lens alignment steps and hence, is more cost-efficient.

3. MEMS LBS ARCHITECTURE

3.1 MEMS mirror

3.1.1 Comparison of scanning methods

For LBS micro-displays, there are two different drawing concepts used, either raster scanning or bi-resonant scanning of the picture, also called Lissajous scanning[28]. The raster scanning method is based on the horizontal axis driven in resonance and the vertical axis driven in a linear motion. The pixel painting can be performed unidirectionally, i.e., only on the horizontal left-to-right scanning of the sine-movement to get more equidistant horizontal lines. In this case, at the horizontal right-to-left movement the lasers are turned off. It is also possible to use a bidirectional horizontal scanning where the pixel painting is performed in both directions as shown in Figure 3(a). The benefit of this method is that the line density is doubled with the drawback that the line density changes from the center to the edges. As clearly visible in Figure 3(a), the density is the highest in the center of the picture and the lowest at the edges. In many practical use cases, the advantages of an increased resolution outweigh the drawback of varying line densities. The second approach for pixel painting in LBS micro-displays is bi-resonant scanning, where the horizontal and the vertical axes are driven in resonance, so both axes are driven in sinusoidal movements which are superimposed to so-called Lissajous trajectories (see Figure 3(b)). The line density can be very high when the ratio between both resonance frequencies is chosen carefully. It has to be mentioned, that the line density for both cases in Figure 3 was highly reduced for illustration purposes. In general, the FOV of MEMS mirrors driven in resonance is higher, so with bi-resonant scanning the typical FOV in the vertical axis is higher. Additionally, the scanning speed of the vertical axis is higher by several order of magnitudes. The drawback of this scanning method is that the line density is much higher in the edges than in the center. Also, the refresh rate is different for each pixel, i.e., some pixels are painted more often than others, strongly depending on the ratio of the two scanning frequencies. To achieve high refresh rates in the center, frequencies above 10 kHz in both axes are typically required.

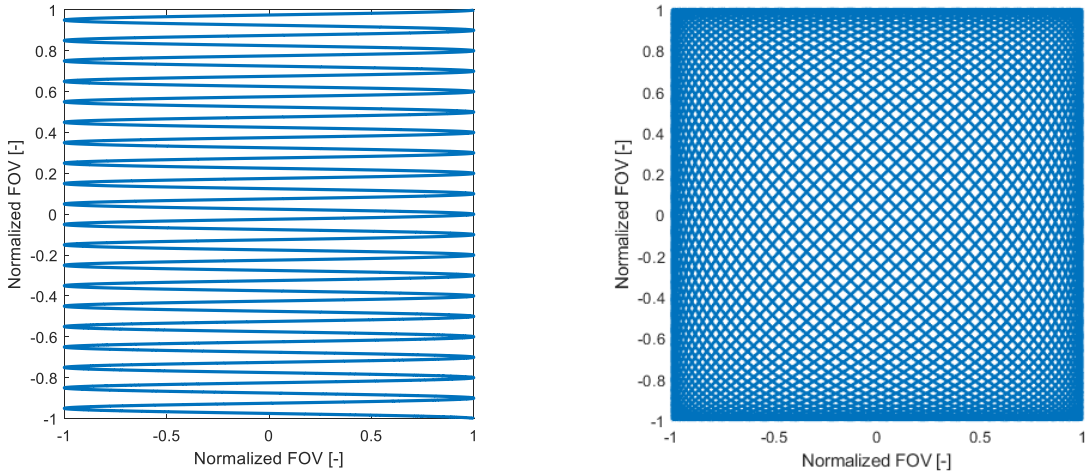

(a) (b)

Figure 3. Comparison of two methods for pixel painting in LBS micro-displays with (a) the raster scanning method where the horizontal axis is driven in resonance and the vertical axis in linear movement and (b) the bi-resonant Lissajous scanning method where both axes are driven in carefully chosen resonance frequencies.

3.1.2 Comparison of mirror configurations

There are two LBS architectures with the main difference being the configuration of the MEMS mirrors. A widely used approach is based on two 1D MEMS mirrors as shown in Figure 4(a)[29]. The first MEMS mirror after the laser module typically has a smaller diameter to provide a high scanning speed of the fast axis. The 1D picture is then delivered to a much larger MEMS mirror which can also be designed elliptical instead of circular to match the beam footprint in that plane. As these second mirrors are much larger in diameter there is a limitation of the scanning speed regarding dynamic deformations and mechanical limitations whereas the first MEMS mirror with the smaller diameter can reach very high scanning frequencies. This demonstrates the advantages and drawbacks at the same time—the high scanning speed of the first and the low scanning speed of the second mirror. Generally, when using raster scanning, the main limitation to achieve

high resolutions in the vertical axis besides the achievable field of view is the high-speed scanning in the horizontal axis of the picture[30]. Here, this architecture is advantageous compared to only one 2D MEMS mirror, illustrated in Figure 4(b). When using bi-resonant scanning instead of raster scanning, high frequencies on both axes showed to have superior results regarding the image composition[28]. Another drawback is the size of the whole system as there are two MEMS mirrors needed which must be aligned within the opto-mechanical tolerances of the system, whereas most systems additionally need relay optics, further increasing size and weight of the optical engine. Furthermore, the driving electronics of an architecture with two 1D MEMS mirrors is typically more complex and larger.

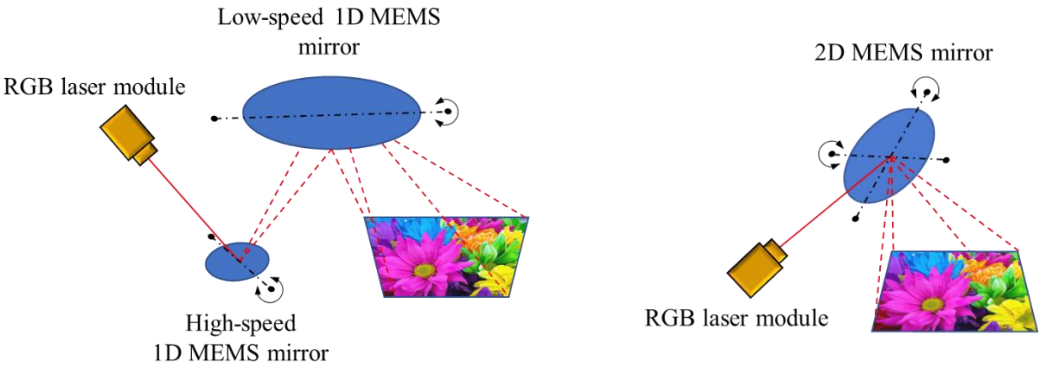

(a) (b)

Figure 4. (a) LBS micro-display architecture based on two separate 1D MEMS mirrors and (b) architecture based on only one 2D MEMS mirror capable of moving independently in two axes. The image distortions are different in both systems and need to be compensated either by pre-processed images or on-the-fly by the TriLite Calibration Module (cf. Section 4.2).

The second main concept of LBS displays is based one 2D MEMS mirror, i.e., the MEMS mirror can be scanned in both axes. The requirements—especially regarding the dynamic deformations and the mechanical suspension—are much higher on those MEMS mirrors and hence, require a careful design. There are two types of 2D MEMS mirrors used in literature, one optimized for raster scanning and one for bi-resonant mode. The first type is optimized for a high frequency in the fast axis (above 10 kHz) and lower frequency in the slow axis (above 60 Hz). The second type is also aiming for higher frequencies above 1 kHz for the slow axis. The main advantage of these systems is that there is only the need of one single MEMS mirror including less alignment steps, typically smaller driving electronics, and lower power consumption. The disadvantages are the possible cross-talk between the two axes. Additionally, higher frequencies are harder to achieve as the diameter of the mirror is larger compared to the first smaller MEMS mirror in LBS displays using 1D MEMS mirrors. However, the benefits with the small footprint on the overall projector size without needing any additional relay optics and the lower power consumption typically outweigh the drawbacks.

3.1.3 Specification of Trixel 2 MEMS mirror

As the Trixel 2 LBS is based on the raster scanning method, the MEMS mirror is optimized for this operation mode, where the resonant fast axis has a frequency of $\approx$ 11 kHz and the quasi-statically actuated slow axis is driven in a modified sawtooth movement with a repetition frequency of 90 Hz. This modified driving signal ensures high linearity and low resonant oscillations of the MEMS mirror due to input shaping of the driving signal[31]. The achievable FOV in the fast axis is 42° (equals a max. mechanical tilting angle of Θ_{mech} = ±10.5°) and in the slow axis 22° (equals Θ_{mech} = ±5.5°). As there are inherent geometric image distortions when using MEMS mirror based LBS displays, in our system these are compensated by the TriLite Calibration Module (cf. Section 4), resulting in an effectively usable FOV of 40° x 20°. In the Trixel 2 architecture a vertical mirror frequency of, e.g., 60 Hz or 90 Hz is targeted to get a flicker-free projection. This means the mirror is able to display approximately 240 or 160 horizontal lines per vertical period, for 60 Hz or 90 Hz, respectively, using both, scanning from the left and the right side. Since the targeted vertical resolution is 480 lines, not all pixels can be refreshed in every vertical MEMS mirror period. A technique similar to interlacing is applied—in two or more periods all pixels are refreshed, depending on the desired vertical frequency. The higher the frequency, the higher the number of periods to refresh all pixels.

3.2 Trixel 2 LBS architecture

The Trixel 2 LBS architecture consists of three main parts: the integrated RGB light module introduced in Section 2, a single 2D MEMS mirror, and a common mounting platform for those two components. The collimation optics included in the laser module are designed so that the outer two laser beams (red and green) exit the light module at an angle α with respect to the blue beam (corresponding to the optical axis of the system). As shown in Figure 5(a), this results in the three RGB beams intersecting at the MEMS mirror plane.

Figure 5(b) depicts the complete LBS after assembly of both laser module and MEMS mirror onto a common mounting platform which is based on the MID technology[32,33], resulting in an injection-molded thermoplastic component with a metallization of electronic circuit traces on its surface. MIDs offer a high degree of flexibility in terms of the complexity of the geometric shape with a relatively low number of process steps, which makes them an interesting technology for LBS systems[34]. Bottom and top view of the MID including 3D circuit tracks are shown in Figure 5(c) and (d), respectively. On the bottom of the MID, a projector PCB for pre-amplification of MEMS position sensing signals is located. The projector PCB also contains a connector for a flexible printed circuit (FPC) for connecting the LBS to the driving mainboard (cf. Section 4).

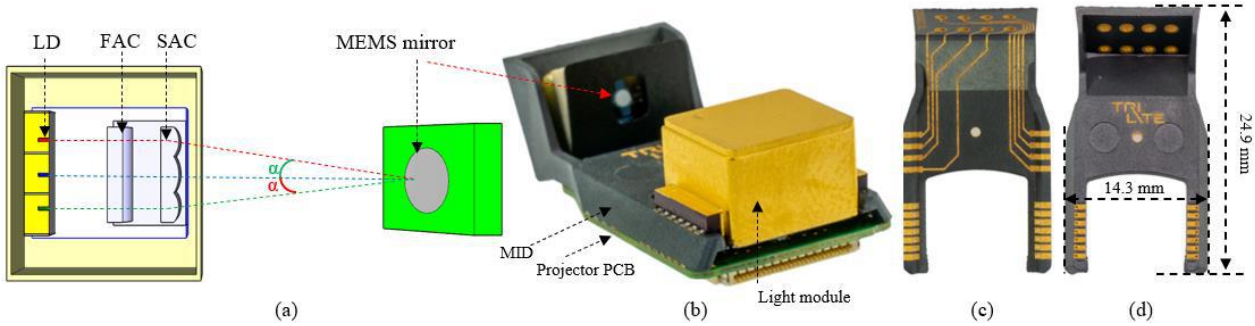

Figure 5. (a) Schematic of laser module and MEMS mirror, (b) LBS after 3D precision assembly of light module, MEMS mirror, and projector PCB onto MID, (c) bottom and (d) top view of the MID.

4. DRIVING ELECTRONICS ARCHITECTURE

4.1 Overview

Figure 6 shows a block diagram of the driving electronics architecture. The mainboard utilizes essentially a field programmable gate array (FPGA), a MEMS mirror driver, a laser diode driver and a non-volatile memory (NVM) storing all projector-individual parameters. A power management section generates all necessary voltages for the digital components, the MEMS driver, and the supply voltages for the three different RGB laser diodes. The three laser diodes have substantially different forward voltages; in order to get a good compromise of dissipated power in the laser driver, modulation speed and setpoint accuracy, the lasers have individual supply rails with different supply voltages. The board is powered via a USB connector. The projector, carrying the light module and the MEMS mirror is connected via an FPC to the mainboard. This cable carries both, all MEMS related signals as well as the laser driving currents. The MEMS position sensing signals are pre-amplified on the projector PCB close to the MEMS in order to prevent electromagnetic crosstalk from the laser driving lines.

With a graphical user interface (GUI) the user can configure a large number of different parameters of the Trixel 2 demonstrator. When the system is powered on, all settings are loaded from the NVM and sent via the controller to the corresponding sections in the system, the demonstrator starts operating and projects an image. The MEMS controller drives, with the help of the MEMS driver, the horizontal MEMS axis in resonance by sensing the mechanical zero-crossing positions. The vertical axis is driven in a quasi-static raster scanning mode. The MEMS controller generates horizontal and vertical synchronization signals to synchronize the TriLite Calibration Module. This module calculates the actual pixel address using these two synchronization signals and the image correction vectors stored in the calibration section of the memory. The TriLite Calibration Module is instantiated for each of the RGB color channels. These three instances are running independently in parallel, i.e., the three colors are projected simultaneously (apart from any color offset corrections

in the time domain). With the calculated pixel addresses (generally different for red, green, and blue) the color information of the corresponding pixel is read from the frame buffer section of the memory and sent to the laser driver as 10-bit values for each color. The user can send test patterns to the frame buffer via the GUI using the USB interface. Alternatively, the user can stream videos via HDMI using any video player.

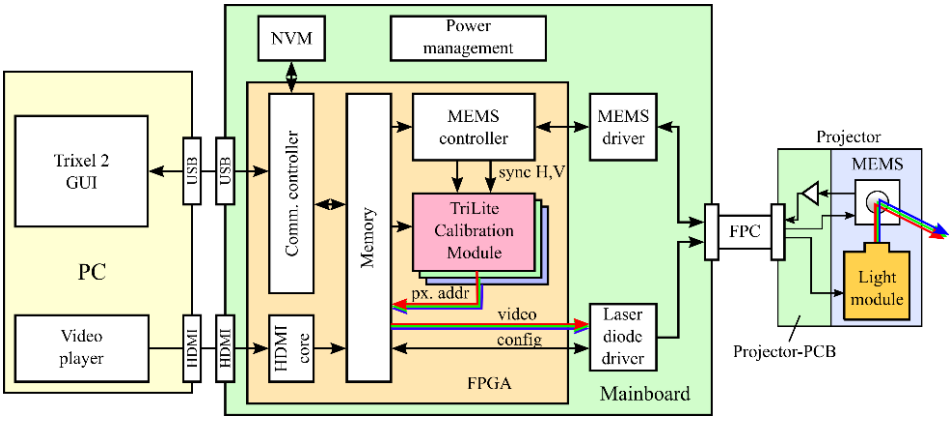

Figure 6. Block diagram of the driving electronics architecture.

4.2 TriLite Calibration Module

MEMS-based LBS systems inherently have geometric image distortions, which the TriLite Calibration Module is capable of correcting by placing the pixels correctly in the time domain. The inputs of this module are the horizontal and vertical synchronization signals, representing, e.g., the mechanical zero-crossing position of the MEMS mirror. Using these signals, the module calculates the pixel address using a correction algorithm. This algorithm is capable of correcting the following typical distortions:

- Geometric distortions inherently caused by MEMS-based LBS as a result of the angle of incident to the mirror and the combination of the two scanning axes (for one 2D or two 1D scanning mirrors, cf. Section 3.1.2)
- Nonlinear beam movement, especially sinusoidal movement when driving one or both MEMS axes in resonance. Also, any deviation from a perfectly linear movement can be corrected.
- Angular offset between the individual laser beams (either caused by placement tolerances and/or by design, as in the architecture presented in this paper, cf. Figure 5(a))
- Transversal offsets of the beams
- Distortions caused by the projection to a screen or caused by any combiner optics

The TriLite Calibration Module uses correction vectors stored in the memory of the system. These vectors are calculated once covering a wide range of opto-mechanical and electronic parameters; like all relevant angles, scanning frequencies and waveforms, shifts, resolution, etc. In case the distortions change (e.g., by aging or temperature-induced), the correction vectors can be recalculated and replaced on-the-fly without interrupting the projection. The module is implemented highly efficient, adding a minimum of logic and electrical power. Once the correction vectors are loaded, the correction runs in real-time with negligible impact on the video-in to retina latency.

The components of the system can be controlled with an interface written in Python. We have developed a library that enables serial communication with the FPGA via an USB-UART interface, which further communicates with the individual components (e.g., laser diode drivers, MEMS mirror driver, temperature sensors on the projector PCB and mainboard). The GUI allows simple control and monitoring of the components and to send image and video information to the LBS. Functions include enabling the software calibration, control the horizontal and vertical MEMS axes, control the driving currents of the laser diodes, manipulate pictures and display a live power and temperature monitor.

5. DEMONSTRATOR DESIGN AND EVALUATION

Figure 7 shows the Trixel 2 demonstrator, which consists of a mainboard, an FPGA module, a projector and connection ports (USB-C, mini-HDMI, mini-USB) as well as the associated projected image and the GUI.

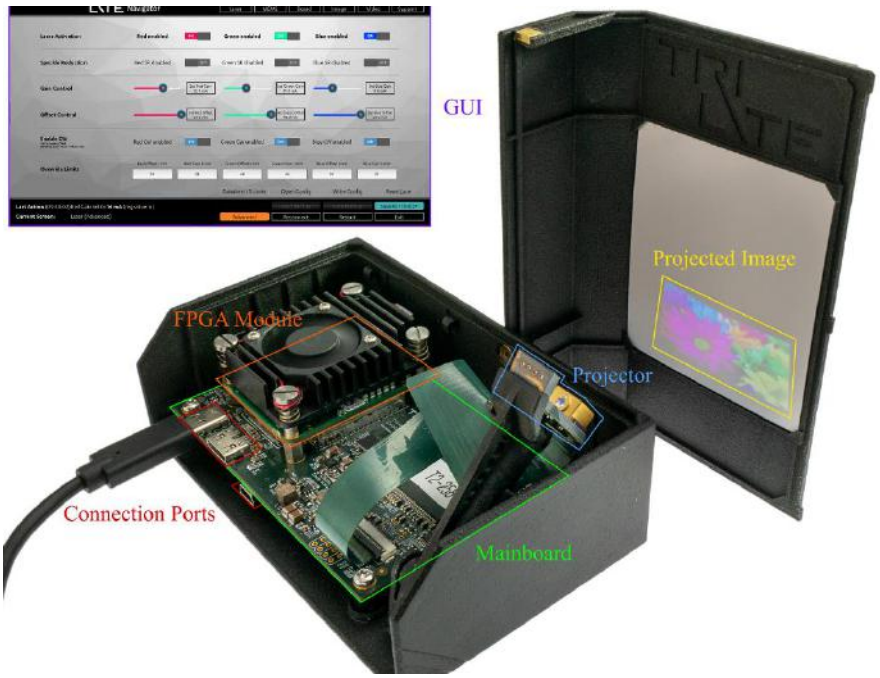

Figure 7. Components of the Trixel 2 demonstrator.

Figure 8 shows test images projected by the Trixel 2 demonstrator. The LBS projects images onto a flat screen with perpendicular angle of incidence and the images are acquired by a camera. The distance between LBS and screen is 50 cm. The LBS and the camera are aligned coaxially in the horizontal plane and as close as possible in the vertical plane without blocking the FOV of the camera.

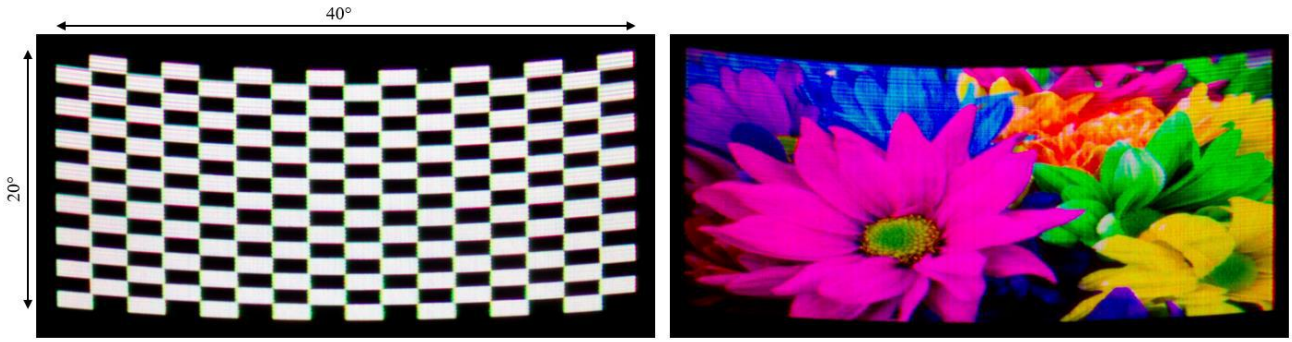

Figure 8. Photos of images projected onto a flat screen: (a) checkerboard test pattern and (b) flower image.

A summary of the main specifications of the LBS presented in this paper is shown in Table 1.

Table 1. Main specifications of the Trixel 2 demonstrator.

Parameter	Trixel 2 specification
Total LBS volume	1.6 cm^3
Total LBS weight	3.1 g
FOV (H x V)	40° x 20°
Resolution (H x V)	960 x 480
Refresh rate	90 Hz, triple interlacing
MEMS mirror type	1 x 2D MEMS mirror
Scanning method	Raster scanning
Projection type	Color simultaneous
Color gamut	230% NTSC RGB
Color depth	3 x 10 bit

6. SUMMARY AND OUTLOOK

All-day wearable and daylight-bright consumer AR devices impose challenging requirements on micro-display engines in terms of size, weight, and image quality. Scanner-based optical engines such as LBS systems offer some unique advantages over panel-based displays in key areas like brightness, contrast, power consumption, FOV, and latency. We have developed an ultra-compact and lightweight LBS targeted for AR applications consisting of an integrated RGB laser module with collimation optics, a single gimballed 2D MEMS mirror, and a hybrid MID/PCB mounting platform.

In this paper, we present the architecture of laser module, LBS scanner, and driving electronics. Conventional RGB laser modules include separately packaged red, green, and blue laser diodes, external collimation optics, and dichroic beam combiners. In our proposed architecture, we assemble the three laser diode dies with sub-µm precision on one common submount and we use only one FAC and one SAC for collimating the laser beams in their fast and slow axes, respectively. All three laser diodes as well as the collimation lenses are enclosed in one single, hermetically sealed package. The collimated RGB laser beams are delivered to the scanning MEMS mirror at different angles of incidence without any RGB beam combiner. Angular offsets between the RGB color channels are compensated with laser pulse timing algorithms integrated in the so-called TriLite Calibration Module. The proposed architecture allows for a substantial reduction in terms of size and weight compared to conventional approaches with RGB beam combiners. In this paper, we present a demonstrator with a FOV of 40° x 20°, an image resolution of 960 x 480 pixels, a refresh rate of 90 Hz (interlaced) with a total LBS volume and weight of 1.6 cm^3 and 3.1 g, respectively.

The architecture of our next-generation LBS is designed from the ground up for consumer AR applications and to be mass manufacturable. It will provide an optimized opto-mechanical interface between LBS and optical combiner with substantial reductions in terms of size and weight, alongside further improvements in terms of FOV, resolution, refresh rate, luminance, and power consumption.[24]

REFERENCES

[1] Zhan, T., Yin, K., Xiong, J., He, Z. and Wu, S.-T., "Augmented Reality and Virtual Reality Displays: Perspectives and Challenges," iScience 23(8), 101397 (2020).

[2] Park, Y. and Murdoch, M. J., "Image quality equivalence between peak luminance and chromaticity gamut," J. Soc. Inf. Disp. 28(11), 854–871 (2020).

[3] Huang, Y., Tan, G., Gou, F., Li, M.-C., Lee, S.-L. and Wu, S.-T., "Prospects and challenges of mini-LED and micro-LED displays," J. Soc. Inf. Disp. 27(7), 387–401 (2019).

[4] Zhan, T., Xiong, J., Zou, J. and Wu, S.-T., "Multifocal displays: review and prospect," PhotoniX 1(1), 10 (2020).

[5] Lee, Y.-H., Zhan, T. and Wu, S.-T., “Prospects and challenges in augmented reality displays,” Virtual Real. Intell. Hardw. 1(1), 10–20 (2019).
[6] Chang, C., Bang, K., Wetzstein, G., Lee, B. and Gao, L., “Toward the next-generation VR/AR optics: a review of holographic near-eye displays from a human-centric perspective,” Optica 7(11), 1563–1578 (2020).
[7] Mi, L., Chen, C. P., Zhang, W., Chen, J., Liu, Y. and Zhu, C., “A retinal-scanning-based near-eye display with diffractive optical element,” presented at Proc.SPIE, 19 February 2020.
[8] Jang, C., Bang, K., Moon, S., Kim, J., Lee, S. and Lee, B., “Retinal 3D: augmented reality near-eye display via pupil-tracked light field projection on retina,” ACM Trans. Graph. 36(6), 1–13 (2017).
[9] Peddie, J., [Augmented Reality: Where We Will All Live, 1st ed. 2017], Springer International Publishing : Imprint: Springer, Cham (2017).
[10] Lin, J., Cheng, D., Yao, C. and Wang, Y., “Retinal projection head-mounted display,” Front. Optoelectron. 10 (2016).
[11] Waldern, J., “Light Engines for XR Smartglasses,” Whitepaper (2020).
[12] Kress, B. C., [Optical Architectures for Augmented-, Virtual-, and Mixed-Reality Headsets], SPIE (2020).
[13] Huang, Y., Liao, E., Chen, R. and Wu, S.-T., “Liquid-Crystal-on-Silicon for Augmented Reality Displays,” Appl. Sci. 8(12) (2018).
[14] Menozzi, M., Bergande, E., Bonan, J., Sury, P. and Krueger, H., “Minimum amount of time required to retrieve peripheral numeric information in augmented-reality systems using a colour sequential DLP display,” Displays 28(2), 85–91 (2007).
[15] Haas, G., “40-2: Invited Paper: Microdisplays for Augmented and Virtual Reality,” SID Symp. Dig. Tech. Pap. 49(1), 506–509 (2018).
[16] Jang, H. J., Lee, J. Y., Kim, J., Kwak, J. and Park, J.-H., “Progress of display performances: AR, VR, QLED, and OLED,” J. Inf. Disp. 21(1), 1–9 (2020).
[17] Huang, Y., Hsiang, E.-L., Deng, M.-Y. and Wu, S.-T., “Mini-LED, Micro-LED and OLED displays: present status and future perspectives,” Light Sci. Appl. 9(1), 105 (2020).
[18] Lee, V. W., Twu, N. and Kymissis, I., “Micro-LED Technologies and Applications,” Inf. Disp. 32(6), 16–23 (2016).
[19] Fidler, F., Balbekova, A., Noui, L., Anjou, S., Werner, T. and Reitterer, J., “Laser Beam Scanning in XR – benefits and challenges,” Proc. SPIE (2021).
[20] Peillard, E., Itoh, Y., Moreau, G., Normand, J.-M., Lecuyer, A. and Argelaguet, F., “Can Retinal Projection Displays Improve Spatial Perception in Augmented Reality?,” 2020 IEEE Int. Symp. Mix. Augment. Real. ISMAR, 80–89, IEEE, Porto de Galinhas, Brazil (2020).
[21] Hedili, M. K., Ulusoy, E., Kazempour, S., Soomro, S. and Urey, H., “Next Generation Augmented Reality Displays,” 2018 IEEE Sens., 1–3 (2018).
[22] Lantian Mi, Chao Ping Chen, Wenbo Zhang, Jie Chen, Yuan Liu, and Changzhao Zhu., “A retinal-scanning-based near-eye display with diffractive optical element,” presented at Proc.SPIE, 19 February 2020.
[23] Reitterer, J., Fidler, F., Schmid, G., Hambeck, C., Julien-Wallsee, F. S., Leeb, W. and Schmid, U., “Software Beam Combiner for Ultra-compact RGB Laser Light Modules with MEMS Mirrors,” Imaging Appl. Opt. 2016, AIW3B.3, Optical Society of America, Heidelberg (2016).
[24] Noui, L., Reitterer, J. and Schöffmann, M., “Laser Beam Scanner and Combiner Architectures,” Proc. SPIE (2021).
[25] “Ultimems.”, 2021, <http://www.ultimems.com/en/index.html>.
[26] “Microvision.”, 2021, <http://www.microvision.com/>.
[27] Reitterer, J., Fidler, F., Schmid, G., Hambeck, C., Julien-Wallsee, F. S., Leeb, W. and Schmid, U., “Integrated RGB Laser Light Module for Augmented and Virtual Reality Applications,” 3.
[28] Hofmann, U., Janes, J. and Quenzer, H.-J., “High-Q MEMS Resonators for Laser Beam Scanning Displays,” 2, Micromachines 3(2), 509–528 (2012).
[29] Holmström, S. T. S., Baran, U. and Urey, H., “MEMS Laser Scanners: A Review,” J. Microelectromechanical Syst. 23(2), 259–275 (2014).
[30] Urey, H., Wine, D. W. and Osborn, T. D., “Optical performance requirements for MEMS-scanner-based microdisplays,” MOEMS Miniaturized Syst. 4178, 176–185, International Society for Optics and Photonics (2000).
[31] Reitterer, J., Fidler, F., Schmid, G., Hambeck, C., Julien-Wallsee, F. S., Leeb, W. and Schmid, U., “Input-shaped actuation of electromagnetic MEMS mirrors,” presented at Proc.SPIE, 21 May 2015.

[32] Ermantraut, E., Zimmermann, A., Müller, H., Wolf, M., Eberhardt, W., Ninz, P., Kern, F. and Gadow, R., "Laser Induced Selective Metallization of 3D Ceramic Interconnect Devices," 2018 13th Int. Congr. Molded Interconnect Devices MID, 1–5 (2018).
[33] Heininger, N., John, W. and Boßler, H.-J., "Manufacturing of molded interconnect devices from prototyping to mass production with laser direct structuring," Int. Congr. MID, 1–20, Citeseer (2004).
[34] Franke, J., "Three-Dimensional Molded Interconnect Devices (3D-MID)," [Three-Dimensional Molded Interconnect Devices (3D-MID)], J. Franke, Ed., Hanser, I–XII (2014).